Article

Developing a p-NDVI Map for Highland Kimchi Cabbage Using Spectral Information from UAVs and a Field Spectral Radiometer

Dong-Ho Lee, Hyoung-Sub Shin and Jong-Hwa Park *

Department of Rural and Agricultural Engineering, Chungbuk National University, 1 Chungdae-ro, Seowon-gu, Cheongju 28644, Chungbuk, Korea; ehdgh3337@naver.com (D.-H.L.); subihoho@hanmail.net (H.-S.S.)
* Correspondence: jhpak7@cbnu.ac.kr; Tel.: +82-43-261-2577

check for updates

Abstract: Kimchi cabbage grows in South Korea and is an essential ingredient for making kimchi with the kimjang method. The technique of accurately managing and monitoring crops such as kimchi cabbage plays an important role in stabilizing consumer prices. Unmanned aerial vehicles (UAVs) are expected to be used more widely in global and local agriculture. The agricultural sites at which kimchi cabbages are cultivated are affected by various climatic, terrain, and soil conditions, requiring technologies that can accurately and quickly acquire such information. UAVs and sensors are able to provide some of these data. In this study, we set up a cultivation environment for kimchi cabbage and investigated the correlation between a UAV-attached multispectral sensor and a field-portable spectroradiometer. Reflectance measurement using a spectroradiometer was performed on 99 kimchi cabbages in a Mt. Maebong testbed. We aimed to find a method for obtaining accurate vegetation information by combining the high spatial and temporal resolution information of the UAV observation with the spectral resolution of the spectroradiometer. Spectral analysis was used to identify the difference between healthy and poorly growing cabbage and to find the wavelength that most affected the growth. The hyperspectrum of the spectroradiometer reflected the accurate vegetation characteristics and contributed greatly to the identification of vegetation indices. A method for correcting the errors that occurred in the ground and UAV monitoring and the difference arising from the application of the broadband wavelength of the UAV and the single wavelength of the spectroradiometer through correlation analysis is presented. The calibration equation method was applied to UAV spatial information and was used to create a precise normalized distribution vegetation index (p-NDVI) map. The p-NDVI map was organized into four categories for the selection of cabbages with healthy (good) growth. Our results show that (1) the merged spectral analysis method was found to be more accurate and distinct than conventional methods, and (2) methods for estimating cabbage growth status showed a higher significant correlation than the UAV-based NDVI. At the maturity stage, high accuracy ($R^2 = 0.7816$, RMSE = 0.06) was achieved for NDVI. Although this map is the result of the limited vegetation monitoring of UAV images taken during the maturity stage, it could be of great help for managing the quality and production of cabbage. However, the efficient management of highland kimchi cabbage requires continuous research under various conditions to enable periodic and systematic monitoring using UAVs and sensors.

Keywords: spectroradiometer; reflectance characteristics; spectral analysis; unmanned aerial vehicle (UAV); multispectral

1. Introduction

In South Korea, kimchi is one of the most important components of the food culture. Kimchi is made in various forms and is consumed throughout the year. The main ingredients of kimchi are kimchi cabbage and radish. The stable production of cabbage is very important because the output of each cabbage period determines consumer prices. Kimjang refers to the process of soaking kimchi, which is performed largely in summer and winter. The production of summer kimchi uses cabbage that grows in high mountainous areas, such as Mt. Maebong. Mt. Maebong has an altitude of 700 to 1250 m above sea level and has the best conditions for growing cabbage during the summer. Mountainous areas with high altitude are relatively cool in summer and have high rainfall and a short sunshine duration. Since mountains and highlands have relatively low temperatures, farmers in these areas raise income by growing vegetables that are suitable for the terrain according to the differences in the temperature and climate according to the altitude of the terrain [1]. Regarding the cultivation of vegetables, there are fewer pests in mountainous areas, and cultivation is more suitable than in flat land areas; thus, vegetables from these areas have the advantage of being able to be shipped when there are market shortages. However, in recent years, the effects of climate change, such as global warming, have strongly affected the production of highland kimchi cabbage, making it difficult to stably produce and ship cabbage [2].

In mid-July, cabbage prices have risen as record heatwaves and droughts have continued in 2018 and 2019 in the Gangwon region, which is the main producer of high-altitude cabbage [3]. The main causes were high temperatures of up to 32.5 °C in mid-to-late July despite yearly average high temperatures of 28 °C, and only 15 mm of precipitation despite the yearly average precipitation of 117 mm. There were around 15 heatwave days in mid- and late July, the highest in the last 25 years. These effects led to poor crops due to disorders such as bruises and calcium deficiency and increased the cost of farming during the heatwave-response process, which contributed to the price rise [4].

On-site monitoring methods for surveying and analyzing alpine vegetables require more time and labor than the methods used on plains. By comparison, the use of unmanned aerial vehicles (UAVs) and sensor systems has the advantage of obtaining high-resolution images quickly and regularly, which is considerably more effective than direct measurements in the field of crop monitoring, such as for planting areas, plant height, growth factors, growth abnormalities, and yield estimation [5–10].

Therefore, the Korean government developed technology to solve the monitoring problem and to prepare supply and demand stability measures by predicting the production volume through the periodic monitoring of the highland cabbage growing area [11–13]. In the past, studies on agricultural land environment observation, crop production, and cultivation-area monitoring have been conducted using satellite imagery, mainly for agriculture [14–20]. In recent years, studies using UAVs have been actively conducted and applied to various agricultural fields [21–24]. A UAV allows the user to acquire agricultural information and super high-resolution and accurate agricultural information at any time from the user's desired location without being heavily constrained by terrain conditions. In South Korea, a number of studies have been conducted investigating the monitoring of crops using UAVs [25,26]. Representative research includes the calculation of onion and garlic cultivation areas [26] and the preparation of high-altitude cabbage-cultivation status maps using UAVs. Kimchi cabbage monitoring provides farmers with useful information to develop farm-management strategies for optimal vegetable production. Na et al. [12,13] analyzed the correlation between the time series of the normalized difference vegetation index (NDVI), meteorological factors, and growth factors using UAV images during the growth period of highland cabbage.

The vegetation index (VI) converts the reflectance, which includes the green, red, and near-infrared (NIR) wavelength bands to which the plant responds, into a scalar non-dimensional variable for information extraction regarding the state of a plant [27]. Observed reflectance is very useful for accurate vegetation information because the target area canopy signal and various data are mixed. Studies on vegetation and soil reflection based on the VI value have been conducted by many researchers [28–34].

In particular, studies minimizing the effect of the soil background on VI have been conducted, using techniques from satellite image processing to UAV images [35].

Currently, images using UAVs are widely used for agricultural observation, but the systematic investigation and theoretical formulation of the plant growth status are still in the early stages. The VI value, due to the difference in the spectral reflection characteristics of plants, is still needed to clearly understand the health status and systematic changes of vegetation [36]. The results obtained in this study will be useful for the generation of a method to adjust the VI for the bias error of the UAV image of a study site. The productivity of cabbages can be more clearly determined using a VI value from which the noise related to soil is removed, as well as through the systematic examination of the growth situation of cabbages.

The aim of this study was to propose a method to determine the growth status of vegetation by utilizing the spatial conceptual relationship between crop growth pattern features and biophysical scene class characteristics using the red and NIR reflectance of the target area and the vegetation coverage.

The purposes of this study were to (1) construct a precision vegetation index (NDVI) map by comparing the UAV-based images during the mature stage of kimchi cabbage and the spectral reflection characteristics obtained with a spectroradiometer and (2) suggest a way to extract the quality of kimchi cabbage using the obtained spatial vegetation monitoring results.

2. Materials and Methods

2.1. Study Area

Mt. Maebong, located in Samsu-dong, Taebaek-si, Gangwon-do, northeastern South Korea (37°07′30″ N, 128°34′30″ E), is 1303 m high (Figure 1). Mt. Maebong is the highest mountain in the north of the country, situated along the Nakdong River in Yeongnam and entering the Hwangji. It is also known as the source of the second-longest river in South Korea, the Nakdong River. The highland cabbage plantation extends from the peak of Mt. Maebong, covering an area of 1.32 million m^2. Kimchi cabbage is also grown in an area of 653,000 m^2 in Guinea Village, which is more than 1000 m above sea level. The cabbage cultivation areas are difficult to observe due to complex topographical conditions, severe slopes, severe winds, and frequent clouds. The Mt. Maebong area has a short period of no frost in summer, and the average temperature in July and August is approximately 20 °C, with a large difference between day and night.
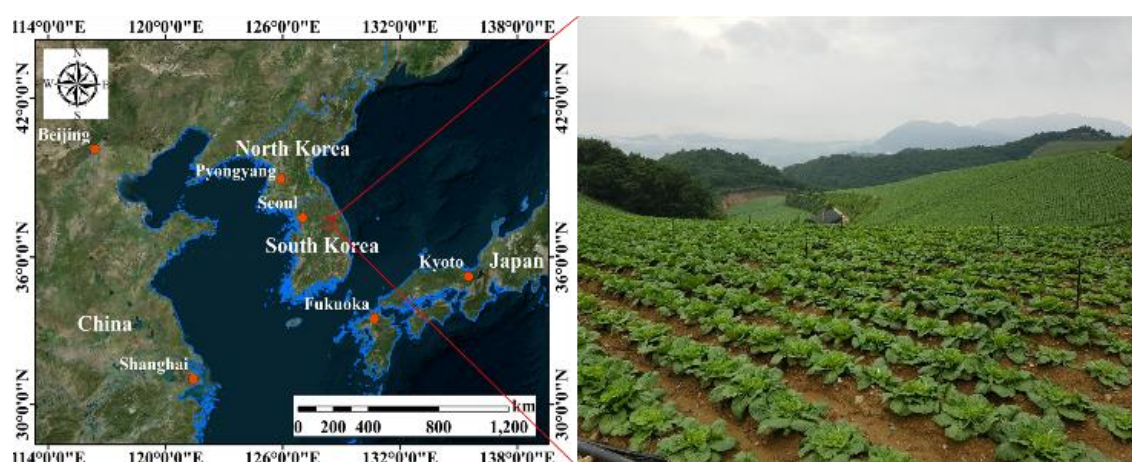

Figure 1. Location map and cultivation status of the study area.

2.2. Kimchi Cabbage Growing Seasons and Growth Calendar

Kimchi cabbage growth differs depending on the variety and cultivation type, but it takes approximately 60 to 120 days from seeding to harvesting. It is a cold-season crop, and its growth

temperature is 15–20 °C. Summer in South Korea is from June to August, and the temperature is usually around 30 °C, which makes it very difficult to grow cabbage. Even at high altitudes, the temperature in the middle of the day is higher than 25 °C in summer, and there are humid conditions, such as sudden showers and fog. These climatic conditions are exacerbated by various diseases that develop under high-temperature and humidity conditions, such as bruises. In order to prevent these disease conditions from occurring, their control is particularly important when growing cabbage. Therefore, systematic monitoring and responses are required to achieve more stable production. Figure 2 shows the cabbage cultivation at the study site.
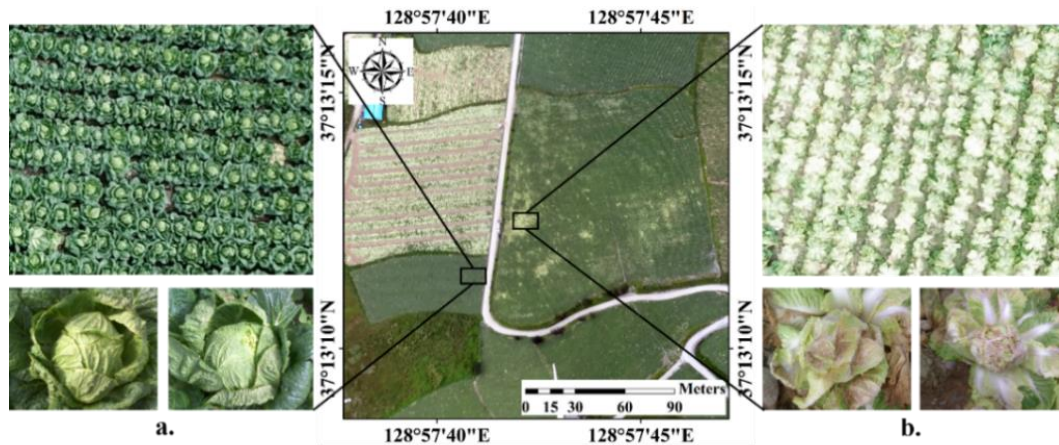

Figure 2. Kimchi cabbage cultivation status at the study site: (**a**). is a case with healthy (good) growth; and (**b**). is a case with unhealthy (poor) growth.

The site survey was conducted from August 11 to 13, 2018. Atmospheric conditions were clear with few clouds. The UAV (eBee; Sensefly, Cheseaux-sur-Lausanne, Switzerland) used was structured as shown in Figure 3. The UAV shooting altitude was 310 m; pictures were taken at a high position to reflect the large features of topographical changes in the mountainous region. The reflectance images photographed under these conditions showed a spatial resolution of 0.11 m. The sensors (S110 NIR; Canon, Tokyo, Japan) and measurement conditions of the UAV are listed in Table 1.
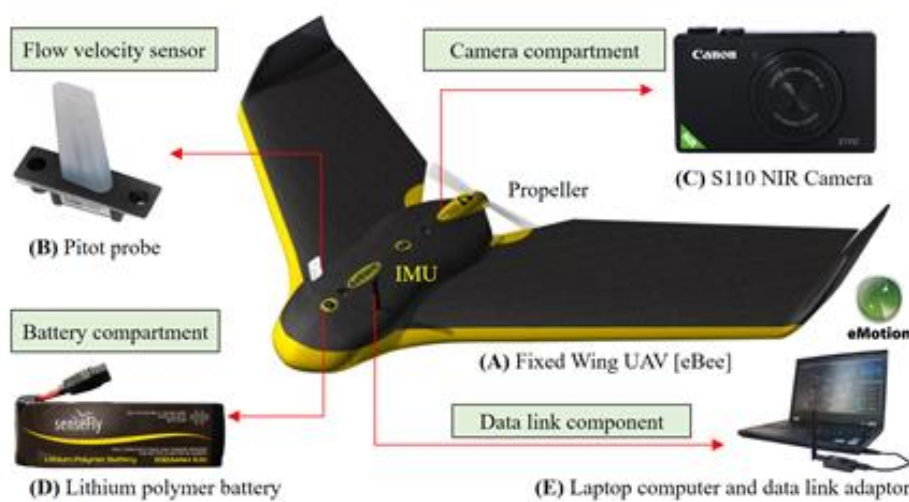

Figure 3. The main components of the unmanned aerial vehicle (UAV) and NIR Sensor.

Table 1. On-site measuring instruments and observation conditions.

Item	Specifications
UAV	e-Bee
Sensor	S110 NIR
Sensor band (nm)	Red (625), Green (550), NIR (850)
Measuring altitude (m)	310
Spatial resolution (m)	0.11
Radiometric resolution	16 bits
Field 1 area (m^2)	13,812
Field 2 area (m^2)	2316

In the field survey, the vegetation indices were calculated by investigating the spectral reflection characteristics using UAV observation and a spectroradiometer (PSR-2500; Spectral Evolution, Haverhill, MA, USA), as shown in Figure 3 and Table 2. Spectral reflection characteristics were measured from four to five cabbage plants using a spectroradiometer for each selected point (Figure 4).

Table 2. Spectroradiometer specifications.

Item	Specifications
Spectroradiometer	PSR-2500
Weight (kg)	3.3
Spectral Range (nm)	350–2500
Spectral Interval (nm)	3.5 (~700)
	20 (~1500)
	18 (~2500)

The total number of measured cabbage plants was 99. Measurement was performed twice per object, and the average value was used. The coordinates of each measuring point were generated using the global positioning system–real-time kinematic (GPS–RTK) system, which improved the position accuracy [35].

The field-portable survey spectroradiometer measured a field of view (FOV) of about 10 cm through the use of an 8° lens. The measurement range of the spectroradiometer was 5 nm intervals from 300 to 1200 nm. In 2018, rainfall was very low, and the hot weather continued; however, the required moisture was supplied through fog, so the entire growing area was deemed to be appropriate for cabbage growth. Therefore, in order to determine the production of cabbage and the characteristics of disease occurrence, and to identify the characteristics associated with the growth status, we selected and examined the location of poor cabbage crop conditions as an experimental point. The survey district was divided into Field 1 and Field 2, as shown in Figure 4. Field 1 had 10 spots with abnormal (poor) growth (X spots) and five spots with healthy (good) growth (triangular spots), while Field 2 had six spots with good growth. Abnormal (poor) growth cabbage shows the softening of cabbage tissue due to the occurrence of wounds, weak or poor drainage, and hot and humid conditions. Healthy (good) growth cabbage shows that the head of the cabbage is well formed at the time of investigation.

2.3. Methods and Research Progression

The research progressed in the following manner.

(1) Selection of target areas and cultivated kimchi cabbages: the target area was selected as Mt. Maebong, a highland cabbage growing area. Cultivated crops were analyzed for the characteristics of cultivation conditions.

(2) Remote sensing (RS)/geographic information system (GIS) data collection: spectral characteristics were investigated using a field-portable survey spectroradiometer (PSR-2500) and a fixed wing UAV (eBee) to collect spatial information in the cabbage cultivation area. On-site UAV

imaging was performed with a multispectral sensor (S110, Cannon, Tokyo, Japan). The acquired images were preprocessed Pix4D Capture and Mapper (Sensefly, Cheseaux-sur-Lausanne, Switzerland) and collected, using data such as the spatial information (location, altitude, area, etc.), to utilize the GIS information [20].

(3) Field survey: since the kimchi cabbage growing state at the time of the survey in 2018 was good, we attempted to compare characteristics by selecting a spot in which the state of the cabbages was not good. On-site surveys were conducted to identify cultivation statuses by checking the site and measurement growth factors to periodically review and supplement the collected data. At this time, the GPS–RTK survey technique was applied to increase the location accuracy of the measuring points. Orthographic images of the cabbage growing state were produced using UAV photographs and ground control points (GCPs).

(4) Comparison of growth-related indices, such as vegetation indices (NDVI, photochemical reflectance index (PRI)): vegetation-related indices using previous research results and UAV image analysis were derived to analyze the field growth status [36,37]. The NDVI and PRI were used to analyze the vegetation conditions in the kimchi cabbage plots of the study area. The PRI is sensitive to the xanthophyll cycle of the carotenoid-based pigments responsible for the heat energy dissipation of plants. It is easy to determine both the photosynthetic ability and physiological stress state of vegetation [38,39]. For the practical use of the UAV, a comparative study was conducted with the field survey data using the field-portable spectroradiometer. Spectral characteristics measured with the UAV and field-portable spectroradiometer were used for the derivation of vegetation indices.

(5) Production of an NDVI map: in order to estimate the growth state of cabbage in the study area, an NDVI map was created according to the cultivation conditions. The correction formula for the production of the precise normalized distribution vegetation index (p-NDVI) map was applied to the field survey using a spectroradiometer.

(6) Result of the review and output of a p-NDVI map: the characteristics of the cultivation status were analyzed, and the NDVI map was corrected by determining the conditions of the spectral reflection characteristics of the field survey results.

Figure 5 shows the flow chart of the implementation process and the methodology of this study. The red dotted boxes on the left represent the indoor work, and the blue dotted boxes on the right represent the on-site survey work process.

2.4. Vegetation Indices

Regarding the research of vegetation indices, more than 70 VIs developed through various RS methods have been proposed and used since 1995 [36]. In particular, the hyperspectral sensor has greatly contributed to VI development by allowing the accurate determination of vegetation characteristics. Hyperspectral data eliminate highly adjacent correlated spectral bands, create a physically meaningful VI, and make it possible to create a new VI that is not sampled as a broadband. However, the wavelength band of sensors that can be used in UAVs is still limited. Therefore, in this study, among the various VIs, two indices (NDVI and PRI) that were verified to reflect the actual vegetation characteristics as a result of existing studies were intensively reviewed. Since the PRI has the optical characteristics of the green wavelength band that NDVI cannot express, we tried to analyze it using the spectroradiometer measurement results. The available evidence shows that the PRI is a reliable estimator of physiological variables closely related to the photosynthetic efficiency at the leaf and canopy levels over a wide range of species, crop functional types, and temporal scales [40].
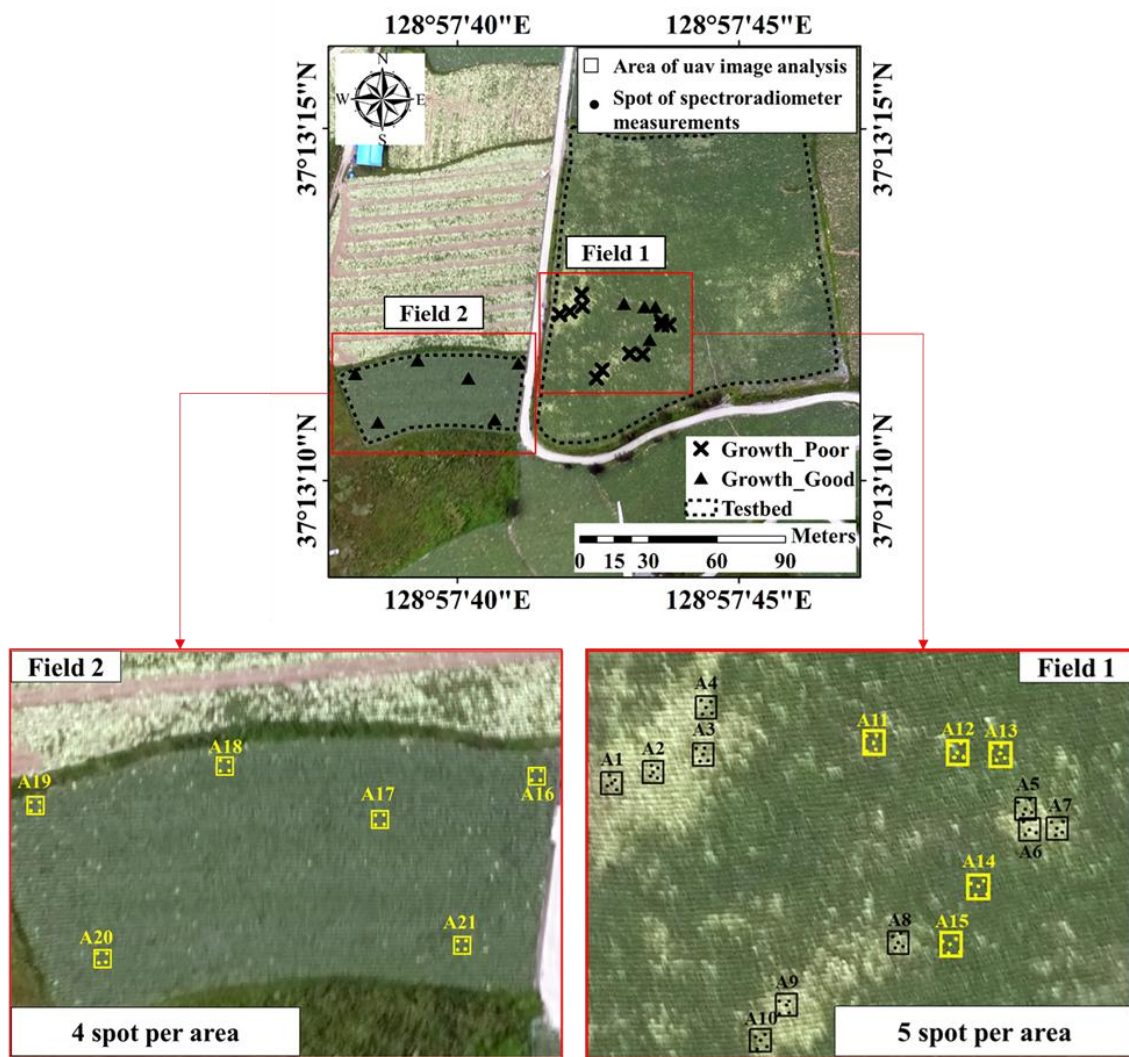
Figure 4. Selection of points for comparison and examination according to kimchi cabbage growth conditions. X points, abnormal growth; triangular points, good growth.

Table 3 shows the vegetation indices, where NIR is the near-infrared wavelength band and red is the visible red wavelength band. NDVI values range from −1 to +1. Rx is the reflectance factor at wavelength x [40–42].

Table 3. Vegetation indices used for the aims of both the broadband and narrowband studies. NDVI: normalized difference vegetation index; and PRI: photochemical reflectance index.

Vegetation Index	Band Type	Equation	Reference
NDVI	Red (625 nm)–NIR (850 nm)	$\frac{NIR - Red}{NIR + Red}$	[40,41]
PRI	Green	$\frac{R531 - R570}{R531 + R570}$	[41]
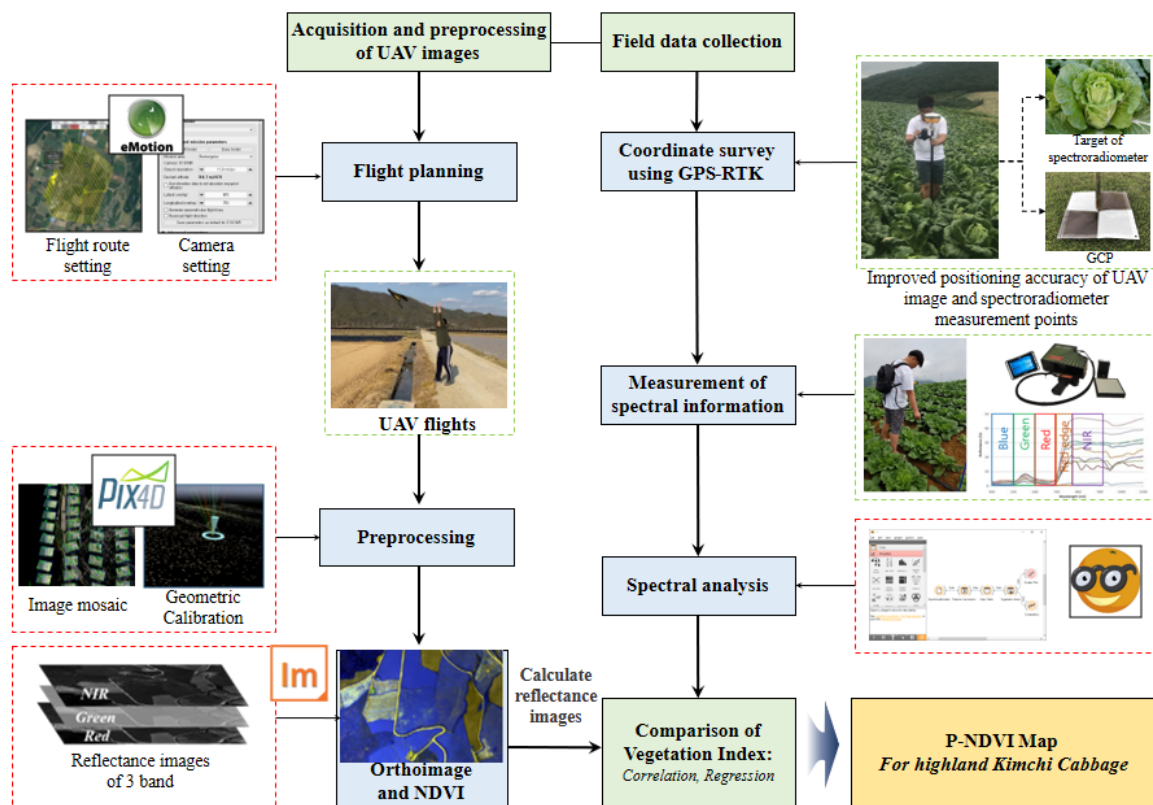
Figure 5. Flowchart of the precise normalized distribution vegetation index (p-NDVI) map calculation process using UAV observations, a spectroradiometer, and global positioning system–real-time kinematic (GPS–RTK) measurements.

3. Results and Discussion

3.1. Terrestrial Spectral Characteristics

In order to realize precision agriculture, detailed crop, soil, and water condition information with a high spatial, spectral, and temporal resolution is required. UAV observations can provide some of this information, but it is often not possible to meet all data requirements with a single sensor observation alone. A spectroradiometer is useful as a complementary method to solve spectral resolution problems and for determining the difference between diseased and healthy spectra, as well as for finding the best and most distinct wavelength band. The spectral analysis method was used to select stepwise variables to identify the wavelength that most strongly affected the spectral characteristics of cabbage. The terrestrial spectral analysis procedure was carried out with the method shown in Figures 4 and 5. The spectral reflection characteristics of cabbage showed a distinct difference between healthy (R1) and unhealthy (R2) individuals, as shown in Figure 6. In the visible wavelength range, the reflectance of the unhealthy kimchi cabbage was higher than that of the healthy cabbage. However, in the near-infrared wavelength range, unhealthy cabbage showed a lower spectral reflectance. In particular, it was found that the spectral reflectance of the near-infrared wavelength was about 20% lower in unhealthy cabbage than in healthy cabbage.

Knowing the characteristics of the change of the slope of the spectral reflection curve of the canopy, it is possible to determine the vegetation information of the canopy. The first derivative method, using the derivative of the spectral reflection curve, is a useful method to determine the wavelength that most affects the growth stage of the canopy based on the spectral slope. Figure 6 (F1 and F2) shows the spectral reflectance according to cabbage growth conditions as a first derivative graph. The first derivative result of the spectral reflectance is useful for removing bands with high correlation from hyperspectral data and finding physically meaningful bands.
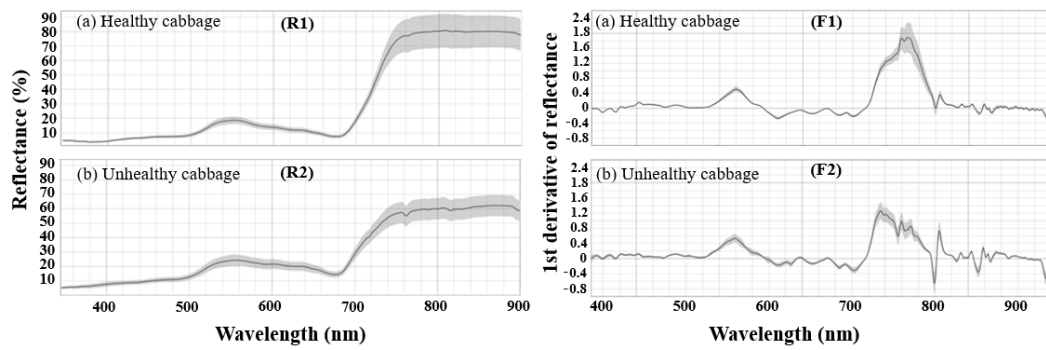
Figure 6. Differences in the spectral reflection characteristics (R1 and R2) and the first derivative of the spectral reflection curve (F1 and F2) between (a) healthy cabbage and (b) unhealthy cabbage.

Figure 7a shows the first derivative of the spectral reflectance of healthy and unhealthy cabbages. As a result of the spectral analysis, there was a reliable difference in the slopes of the reflectance between the three wavelength regions. Figure 7b,c compare the differences between healthy and unhealthy cabbages in the three wavelength bands in which the change in the spectral reflection characteristics of cabbage was the greatest. First, in Figure 7b, there are differences in the range of from about 510 to 530 and 570 nm corresponding to the green wavelength. In the green band range, the reflectance slope graph of the healthy cabbage is steeper than that of the unhealthy cabbage. It can be confirmed that the growth condition of cabbage is highly correlated with PRI, as shown in Table 3.
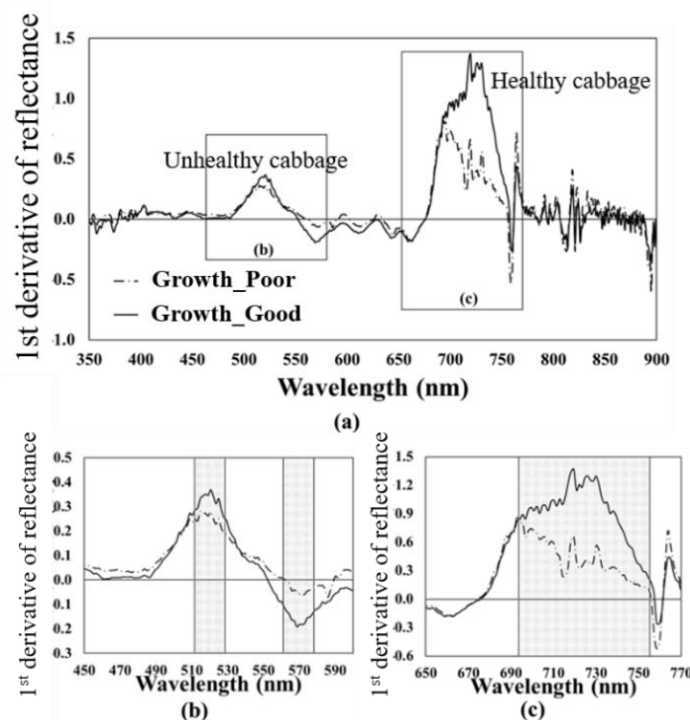
Figure 7. Comparison of the first derivative of the spectral reflectance of healthy and unhealthy cabbages based on wavelength. (**a**) Figures show that the wavelengths between 450–600 nm (**b**) and 650–770 nm (**c**) were most sensitive to PRI and chlorophyll status detection.

Second, in Figure 7c, a difference occurred between about 690 and 750 nm. This range corresponds to the red edge wavelength, in which the reflectance rapidly increases between red and near-infrared wavelengths. The red edge wavelength is known to be useful for the evaluation of chlorophyll status

and leaf area index [43] and was found to be a useful wavelength band for determining the growth condition of cabbage. The health status of cabbage was found to show a large variation at this point.

3.2. Reflectance Characteristics of UAV Imagery

Figure 8 shows the relationship between the broadband band image acquired by the UAV-equipped sensor and the hyperspectral image acquired by the spectroradiometer. The spectral characteristics show a certain variation relationship between the healthy and unhealthy cabbages in the same data acquisition wavelength range of the two sensors.
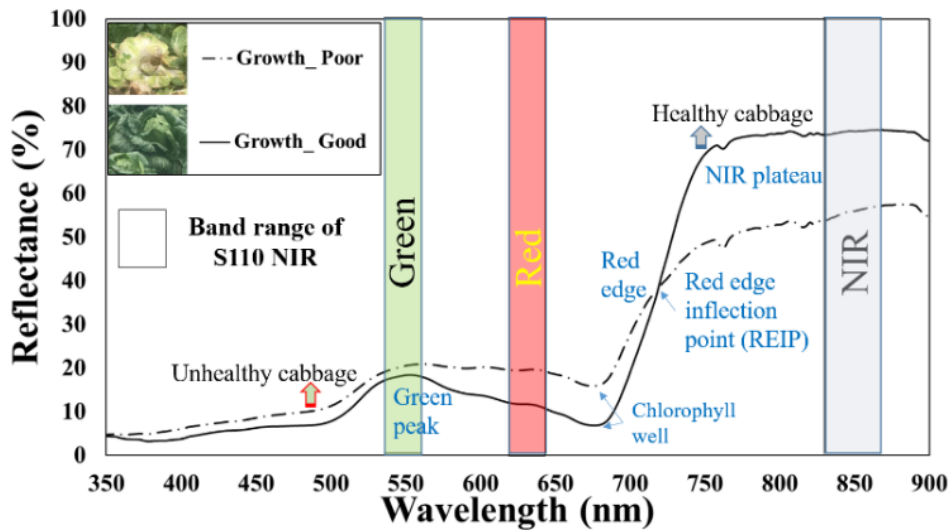
Figure 8. Comparison of the hyperspectral reflection characteristics of healthy and unhealthy cabbages and the wavelength range of data acquired by a UAV imaging sensor.
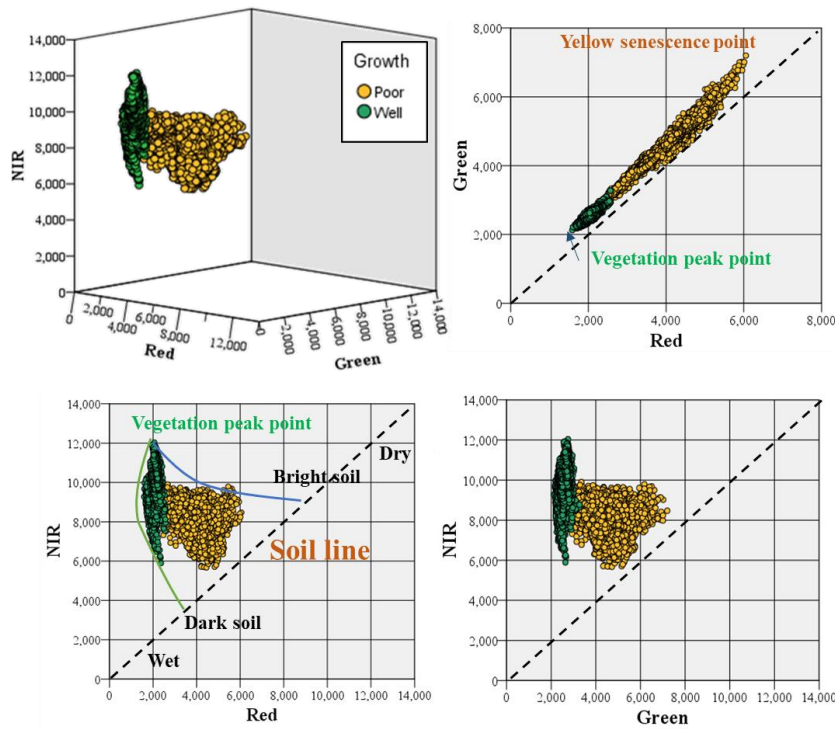
Figure 9. Three-dimensional distribution of green, red, and near-infrared wavelengths of healthy and unhealthy cabbages and the correlation of each band identified by the UAV imaging sensor.

For this feature, the correlation of each band was analyzed using the image acquired by UAV, as shown in Figure 9. As a result of UAV image processing, a reflectance image with a digital number (DN) value in the range of 1–65,535 was shown. The 3D scatter plot was analyzed to confirm the distribution of the DN values of healthy and unhealthy cabbage for the three bands. In the case of red and green bands, the difference between the two cases was obvious. The DN value of healthy cabbage was lower than 3000, but that of the unhealthy cabbage was higher than 3000. The obtained result clearly expressed the tasseled cap feature, which was expressed as a soil line in the relationship between the red and NIR bands.

Figure 10 shows the correlation between the bands obtained using a spectroradiometer. The results obtained using the UAV and spectroradiometer showed almost similar trends. Therefore, in this study, in order to utilize spatial information using UAV images, we attempted to increase the precision by applying the values obtained from the spectroradiometer.
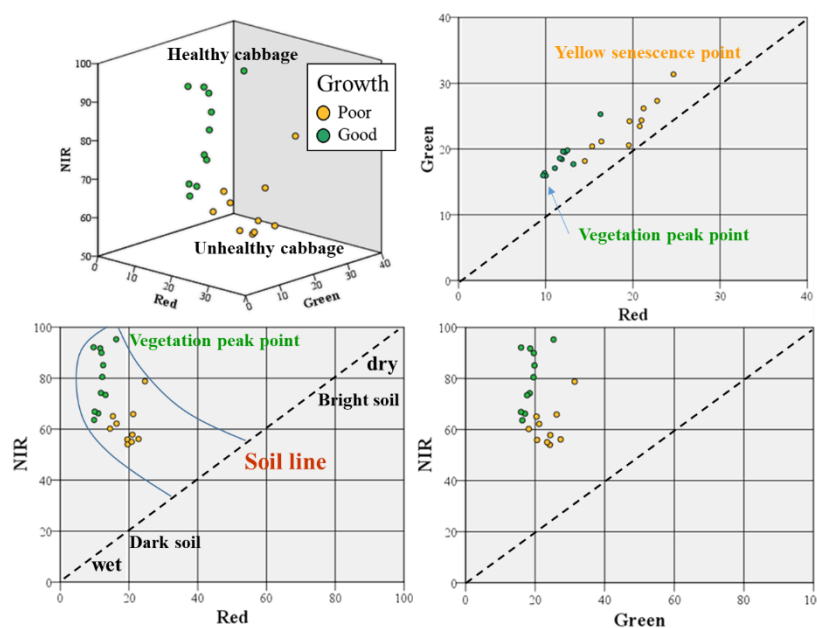

Figure 10. Three-dimensional distribution of the green, red, and near-infrared wavelengths of healthy and unhealthy cabbages and the correlation of each band identified by the spectroradiometer.

As a result of comparing the UAV-mounted-sensor and field-portable spectroradiometer spectrum information, the red sensor values showed the highest correlation in the three bands; the NIR band showed an intermediate correlation, and the green wavelength showed the lowest correlation (Figure 11). These results show that it is useful to use red and near-infrared wavelengths along with the vegetation index. Therefore, this study focused on the NDVI, which expressed both wavelengths well.

3.3. Vegetation Indices of UAV Imagery and the Spectroradiometer

The geospatial information acquisition point had a variety of growth conditions compared to the growth conditions of other sites. Since the sensor used in this study employed green, red, and near-infrared wavelengths, the growth status of cabbage was analyzed using the optimized NDVI.

Figure 12 is an NDVI map made with a combination of red and near-infrared wavelength images acquired by the UAV. As shown in Figure 13, the NDVI showed a mean value of 0.6 or more in a healthy growth state, but a mean value of 0.4 or less in the poor state. Furthermore, healthy cabbage cultivation regions showed very homogeneous NDVI values, but cabbage regions with poor growth had various low NDVIs. According to the cabbage canopy condition, the NDVI was divided into healthy and unhealthy at a value of approximately 0.5 (minimum value) in terms of the conditions ahead of the harvest time. Healthy and well growing cabbage had a value higher than 0.5 (minimum

value) for the NDVI, and most of the poor growing cabbage had a value lower than 0.5. The obtained results are interpreted to reflect the characteristics of healthy cabbage, showing increased near-infrared reflectance in the spectral reflection curve of Figure 8 but decreased reflectance in the visible band.
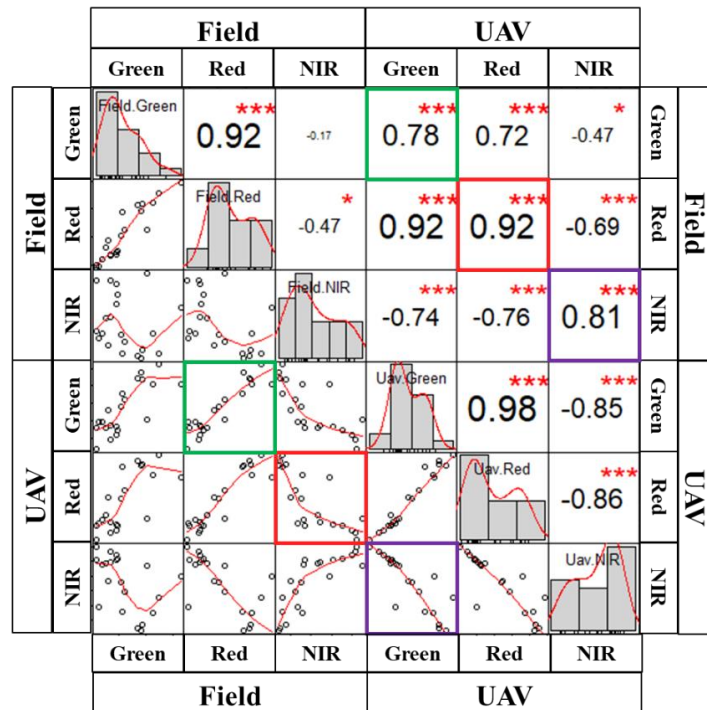

Figure 11. Correlation between the UAV images and on-site spectroradiometer survey results for each band. The number of * represents the level of correlation, *** represents high correlation, * represents low correlation.
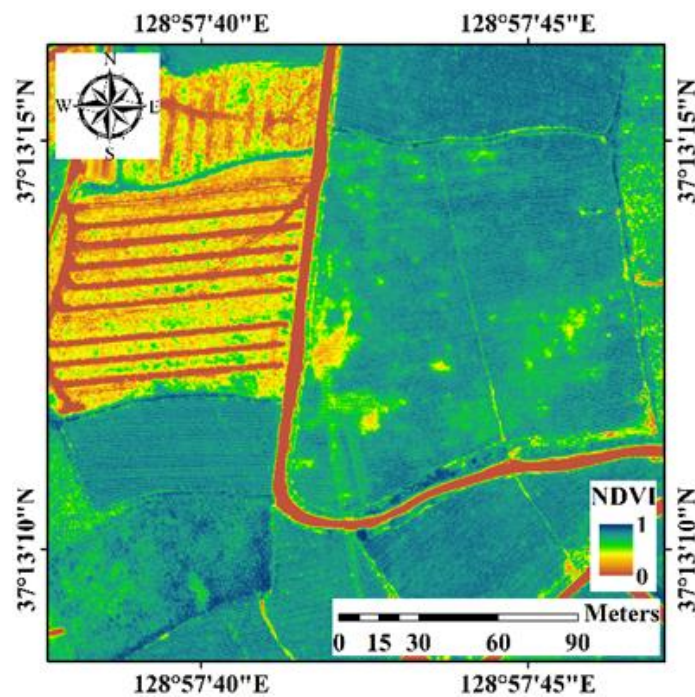
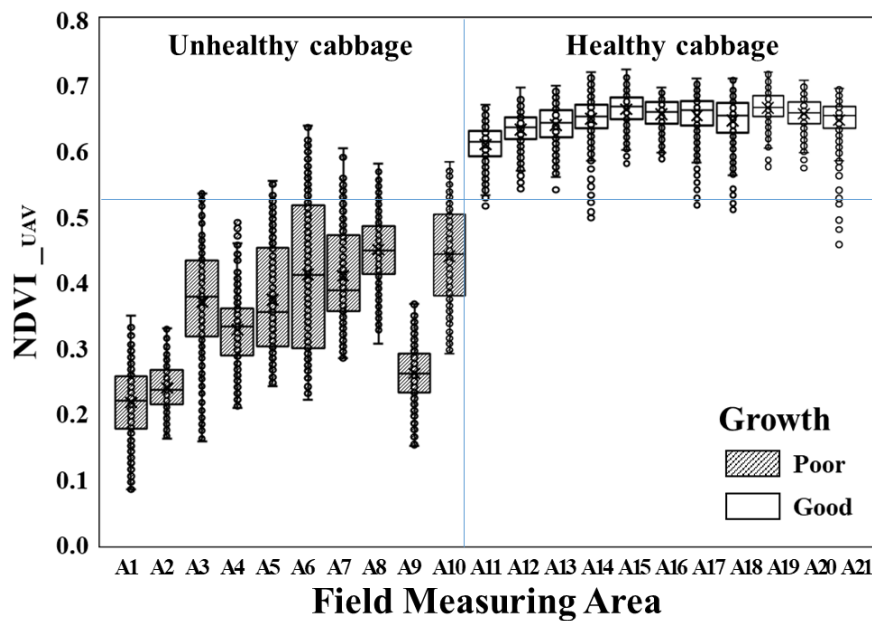**Figure 12.** NDVI spatial distribution in images acquired by the UAV.

Figure 13. Comparison of NDVI according to growth conditions using UAV imagery.

Figure 14 shows the NDVI and PRI obtained using the spectroradiometer. According to the growth conditions using the spectroradiometer, the NDVI had values of around 0.67 for the healthy, well growing cabbage. On the other hand, unhealthy cabbage had an NDVI of about 0.52, reaching as low as 0.15. As a result, healthy cabbages showed very uniform NDVI values, but cabbages with poor growth showed various low NDVIs according to poor growth conditions. The NDVI obtained using the spectroradiometer was 0.15 higher than the value obtained with the UAV.
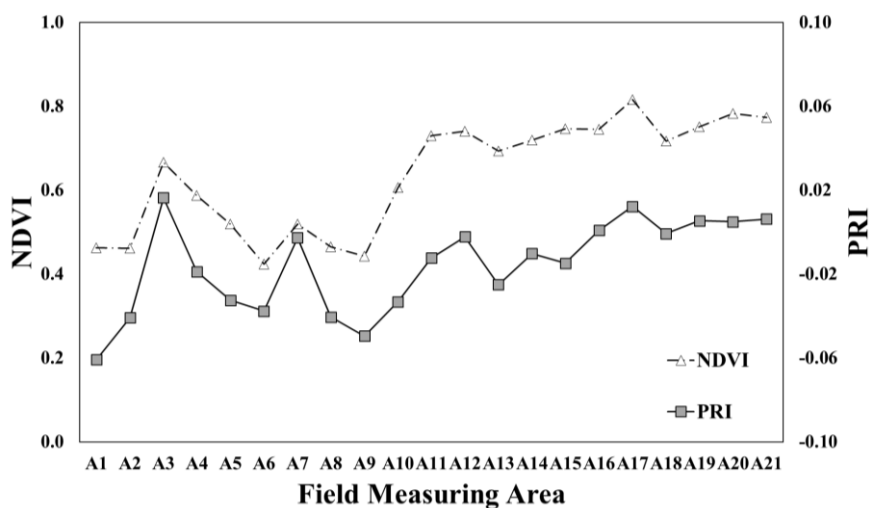

Figure 14. Comparison of NDVI and PRI obtained using a spectroradiometer according to the growth status of cabbage.

The PRI was analyzed to identify the characteristics of the wavelength variation observed in the green band in Figure 7b. The PRI tended to show positive values for the cabbages with good growth but negative values for cabbages with poor growth. These findings are in good agreement with those of Garbulsky et al. [38]. Therefore, while cabbage exhibits a healthy growth state, it shows a sensitive response to light, whereas for cabbage in a poor state, the reaction to light cannot be properly performed.

The NDVI and PRI measured using the spectroradiometer showed a positive correlation, as shown in Figure 15. These results were homogeneous and showed a remarkable correlation with better growth conditions. This characteristic is interpreted as showing that a stable variation in the near-infrared band indicates the health status of cabbage. Cabbage with healthy growth exhibited a positive PRI value, and the NDVI converged to a constant value close to 1. On the other hand, cabbages with poor growth showed a non-homogeneous characteristic because their spectral characteristics increased in the visible wavelength and were very low in the near-infrared band depending on their health status.
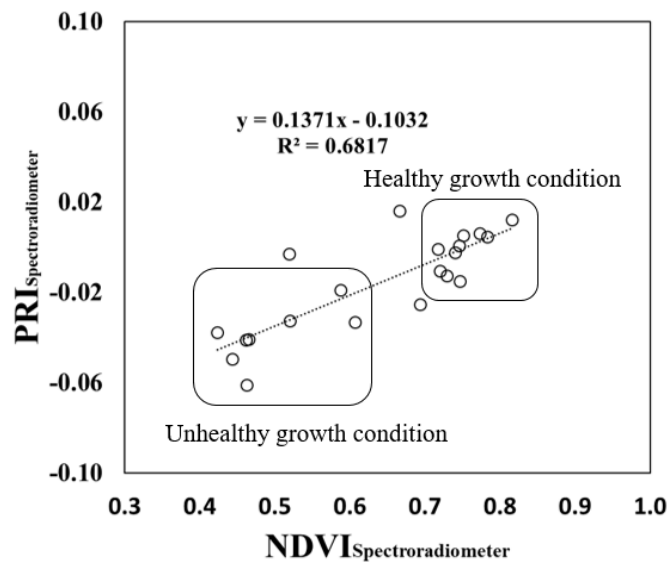

Figure 15. Correlation between NDVI and PRI obtained using a spectroradiometer.

3.4. Comparison of UAV- and Spectroradiometer-Measured NDVI

The NDVI obtained using the UAV sensor and field spectroradiometer showed a constant positive correlation, as shown in Figure 16. The NDVI based on UAV was found to be between 0.1 and 0.2 lower than that of the field survey. This difference is the result of applying a broadband wavelength to the UAV at the two applied wavelengths and applying a single wavelength to each of the red and near-infrared wavelengths of the spectroradiometer.
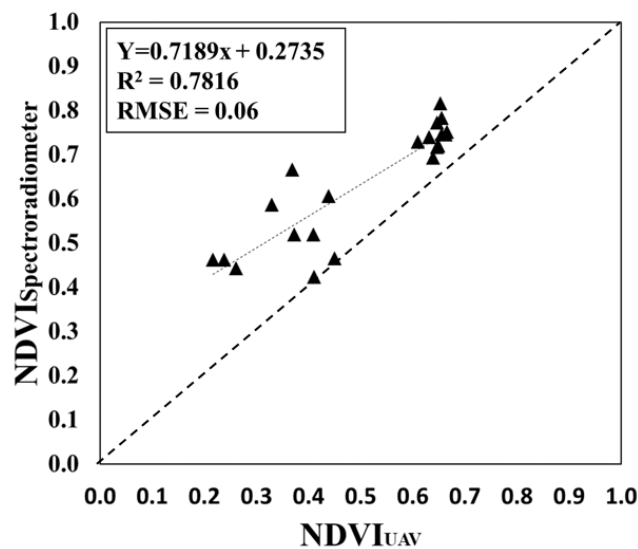

Figure 16. Comparison of NDVI using the UAV and spectroradiometer.

The NDVI measured with the UAV was lower than the field-measured NDVI and was calibrated by applying the relational formula shown in Figure 16.

Regarding the UAV imagery before calibration under the conditions at harvest time, the NDVI values were classified into healthy (good) and unhealthy (poor) growth based on a value of approximately 0.5. After calibration, the NDVI was bound at 0.67, i.e., an increase of about 0.17 (Figure 17). The NDVI measured with the UAV was lower than the field-measured NDVI before calibration, but after calibration, the NDVI frequency shifted to a pattern similar to that obtained under field conditions, as shown in Figure 18.
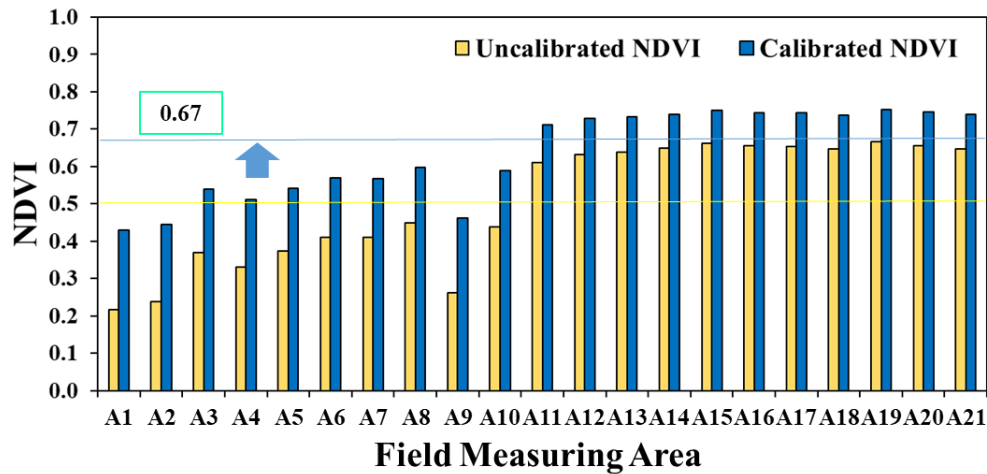

Figure 17. Comparison of UAV imagery NDVI before and after calibration. The yellow line is the boundary value before calibration, and the blue line is the boundary value after calibration.
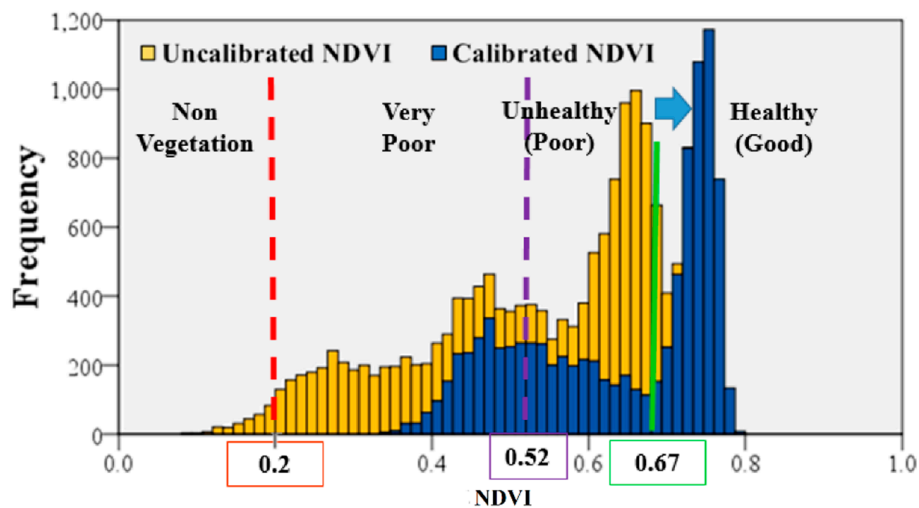

Figure 18. NDVI frequency shift before and after the calibration of NDVI measured by the UAV.

3.5. Creating a p-NDVI Map

Accurate vegetation information taking into account the production volume and product value of cabbage is useful for providing quality products to consumers as well as for ensuring farmers' income and estimating the accurate supply. In this study, in order to create a p-NDVI map, healthy cabbages (NDVI ≥ 0.67) with a high product value and poor growth conditions (poor: 0.52 < NDVI < 0.67, very poor: 0.2 < NDVI < 0.52) and facilities (NDVI < 0.2), such as roads and soil, were classified into four categories. Figure 19 shows the produced p-NDVI map and the status of each category.

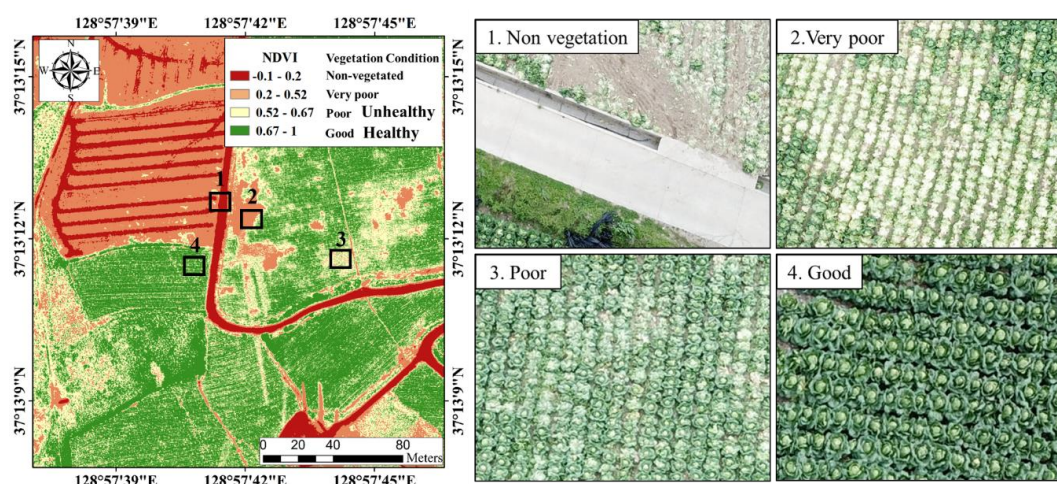**Figure 19.** p-NDVI map according to the vegetation distribution (left) and cabbage status in each category (right).

The p-NDVI map is intended to express the site conditions as well as possible by using the NDVI for each individual cabbage measured in the field with the spatial information (NDVI) obtained by the UAV. It was confirmed that the resulting p-NDVI reflected the field conditions very well. In the future, it will be necessary to develop a method that can provide information rapidly with minimal shooting, taking into account the temporal restrictions that occur in mountainous terrain conditions and restrictions due to climatic conditions.

The results obtained in the future are expected to be useful for predicting the production volume of cabbage, which has a great influence on consumer prices in South Korea.

4. Conclusions

In South Korea, it is very difficult to obtain high-quality satellite images based on the growing stage of cabbage because of the complex topography and weather conditions, such as the rainy seasons and narrow farmland areas. In order to evaluate the crop condition of cabbage, it is essential to secure time-series image data according to the growing season of the cabbage. However, although South Korea's satellite technology has continuously developed, there are many difficulties in securing stable images for use. In this respect, UAVs have a narrow shooting range but are influenced relatively little by weather and can shoot cabbage farmland at any time; thus, they can overcome the shortcomings of other platforms. In addition, due to rapid technological development, UAVs have the advantage of being able to collect images relatively inexpensively with a high resolution of around 10 cm. Therefore, a UAV can be used to evaluate crop conditions under various levels of cultivation complexity with a field size of 1~10 km^2, such as highland cabbage.

The crop conditions of highland cabbages vary according to weather changes and have an effect on the supply and demand of cabbages, which is an important cause of price instability. Therefore, a stable supply and demand of highland cabbage and a reasonable farming plan require scientific, rapidly acquired, and accurate crop information. This study was conducted to monitor the growth status of kimchi cabbage. Highland kimchi cabbage is cultivated in high mountainous terrain areas with relatively low summer temperatures, making it difficult to monitor regularly. This study presented a method for creating a p-NDVI map using a UAV and field survey data for Mt. Maebong, which plays an important role as a highland cabbage cultivation area.

UAV observation provides high spatial and temporal resolution information, but it is often not possible to provide all vegetation information with limited sensors. In order to compensate for this problem, this study attempted to identify the difference between healthy cabbage and poorly growing cabbage and to find the most distinct wavelength band through spectrum analysis using a

spectroradiometer. The spectral analysis method was used to select stepwise variables to identify the wavelength that most affected the growth characteristics of cabbage. The first derivative result of the spectroradiometer was used as a vegetation index by removing bands with a high correlation from the hyperspectral data and finding a physically meaningful band. The spectral reflection characteristics of cabbage were used to determine the difference between healthy and unhealthy cabbages by identifying the wavelength band with the largest change between green and NIR. In particular, the hyperspectrum of the spectroradiometer reflected accurate vegetation characteristics and greatly contributed to the search for vegetation indices. The characteristic wavelength was used to generate the NDVI and PRI.

In the red and near-infrared wavelengths under the same conditions, the difference arising from the application of the broadband wavelength of the UAV and the single wavelength of the spectroradiometer was calibrated through correlation analysis. The correction equation was applied to UAV spatial information and was used to create a p-NDVI map. The p-NDVI map was organized into four categories so that it could be used for the selection of cabbages with good growth. This map could help to manage the quality and production of cabbage as a result of the limited vegetation monitoring of UAV images collected during the mature stage of cabbage.

In the future, it will be necessary to review and supplement more diverse conditions through continuous research.

References

1. Ahn, J.-H.; Kim, K.-D.; Lee, J.-T. Growth Modeling of Chinese Cabbage in an Alpine Area. *Korean J. Agric. For. Meteorol.* **2014**, *16*, 309–315. [CrossRef]

2. Park, J.Y.; Park, Y.G. *The Development of Chinese Cabbage and Radish Forecast Models*; Other Research Reports M125; Korea Rural Economic Institute (KREI): Naju, Korea, 2013; pp. 4–24. ISBN 978-89-6013-588-8 93520.

3. Korea Rural Economic Institute (KREI). 2019. Available online: http://aglook.krei.re.kr/jsp/pc/front/observe/monthlyReport.jsp (accessed on 30 June 2019).

4. Kang, S.-M.; Kim, J.-T.; Hamayun, M.; Hwang, I.-C.; Khan, A.L.; Kim, Y.; Lee, J.-H.; Lee, I.-J. Influence of prohexadione-calcium on growth and gibberellins content of Chinese cabbage grown in alpine region of South Korea. *Sci. Hortic.* **2010**, *125*, 88–92. [CrossRef]

5. Ballesteros, R.; Ortega, J.F.; Hernandez-Lopez, D.; Moreno, M.A. Applications of georeferenced high-resolution images obtained with unmanned aerial vehicles. Part I: Description of image acquisition and processing. *Precis. Agric.* **2014**, *15*, 579–592. [CrossRef]

6. Li, L.; Zhang, Q.; Huang, D. A Review of Imaging Techniques for Plant Phenotyping. *Sensors* **2014**, *14*, 20078–20111. [CrossRef]

7. Zhou, X.; Zheng, H.; Xu, X.; He, J.; Ge, X.; Yao, X.; Cheng, T.; Zhu, Y.; Cao, W.; Tian, Y. Predicting grain yield in rice using multi-temporal vegetation indices from UAV-based multispectral and digital imagery. *ISPRS J. Photogramm. Remote Sens.* **2017**, *130*, 246–255. [CrossRef]

8. Roth, L.; Streit, B. Predicting cover crop biomass by lightweight UAS-based RGB and NIR photography: An applied photogrammetric approach. *Precis. Agric.* **2017**, *19*, 93–114. [CrossRef]

9. Zheng, H.; Cheng, T.; Zhou, M.; Li, D.; Yao, X.; Tian, Y.; Cao, W.; Zhu, Y. Improved estimation of rice aboveground biomass combining textural and spectral analysis of UAV imagery. *Precis. Agric.* **2018**, *20*, 611–629. [CrossRef]

10. Jiang, Q.; Fang, S.; Peng, Y.; Gong, Y.; Zhu, R.; Wu, X.; Ma, Y.; Duan, B.; Liu, J. UAV-Based Biomass Estimation for Rice-Combining Spectral, TIN-Based Structural and Meteorological Features. *Remote Sens.* **2019**, *11*, 890. [CrossRef]

11. Na, S.; Lee, K.; Baek, S.; Hong, S. Estimation of Chinese Cabbage Growth by RapidEye Imagery and Field Investigation Data. *Korean J. Soil Sci. Fertil.* **2015**, *48*, 556–563. [CrossRef]

12. Na, S.-I.; Hong, S.-Y.; Park, C.-W.; Kim, K.-D.; Lee, K.-D. Estimation of Highland Kimchi Cabbage Growth using UAV NDVI and Agro-meteorological Factors. *Korean J. Soil Sci. Fertil.* **2016**, *49*, 420–428. [CrossRef]

13. Na, S.-I.; Park, C.-W.; Lee, K.-D. Application of Highland Kimchi Cabbage Status Map for Growth Monitoring based on Unmanned Aerial Vehicle. *Korean J. Soil Sci. Fertil.* **2016**, *49*, 469–479. [CrossRef]

14. Tsiligirides, T. Remote sensing as a tool for agricultural statistics: A case study of area frame sampling methodology in Hellas. *Comput. Electron. Agric.* **1998**, *20*, 45–77. [CrossRef]

15. Yang, C.; Everitt, J.H.; Bradford, J.M. Comparison of QuickBird Satellite Imagery and Airborne Imagery for Mapping Grain Sorghum Yield Patterns. *Precis. Agric.* **2006**, *7*, 33–44. [CrossRef]

16. Zhao, D.; Huang, L.; Li, J.; Qi, J. A comparative analysis of broadband and narrowband derived vegetation indices in predicting LAI and CCD of a cotton canopy. *ISPRS J. Photogramm. Remote Sens.* **2007**, *62*, 25–33. [CrossRef]

17. Zhang, C.; Guo, X. Monitoring northern mixed prairie health using broadband satellite imagery. *Int. J. Remote Sens.* **2008**, *29*, 2257–2271. [CrossRef]

18. Wang, K.; Franklin, S.E.; Guo, X.; Cattet, M.R.L. Remote Sensing of Ecology, Biodiversity and Conservation: A Review from the Perspective of Remote Sensing Specialists. *Sensors* **2010**, *10*, 9647–9667. [CrossRef]

19. Na, S.-I.; Park, J.-H.; Park, J.-K. Development of Korean Paddy Rice Yield Prediction Model (KRPM) using Meteorological Element and MODIS NDVI. *J. Korean Soc. Agric. Eng.* **2012**, *54*, 141–148. [CrossRef]

20. Xiong, D. Crop Growth Remote Sensing Monitoring and its Application. *Sens. Trans.* **2014**, *169*, 174–178. Available online: https://sensorsportal.com/HTML/DIGEST/april_2014/Vol_169/P_PR_0110.pdf (accessed on 24 August 2020).

21. Park, J.K.; Park, J.H. Applicability Evaluation of Agricultural Subsidies Inspection Using Unmanned Aerial Vehicle. *J. Korean Soc. Agric. Eng.* **2016**, *58*, 29–37. [CrossRef]

22. Park, J.K.; Park, J.H. Analysis of Rice Field Drought Area Using Unmanned Aerial Vehicle (UAV) and Geographic Information System (GIS) Methods. *J. Korean Soc. Agric. Eng.* **2017**, *59*, 21–28. [CrossRef]

23. Toscano, P.; Castrignanò, A.; Di Gennaro, S.F.; Vonella, A.V.; Ventrella, D.; Matese, A. A Precision Agriculture Approach for Durum Wheat Yield Assessment Using Remote Sensing Data and Yield Mapping. *Agronomy* **2019**, *9*, 437. [CrossRef]

24. Na, S.I.; Park, C.W.; So, K.H.; Ahn, H.Y.; Lee, K.D. Application method of unmanned aerial vehicle for crop monitoring in Korea. *Korean J. Remote Sens.* **2018**, *34*, 829–846. [CrossRef]

25. Park, J.-K.; Das, A.; Park, J.-H. Application trend of unmanned aerial vehicle (UAV) image in agricultural sector: Review and proposal. *Korean J. Agric. Sci.* **2015**, *42*, 269–276. [CrossRef]

26. Lee, K.-D.; Lee, Y.-E.; Park, C.-W.; Na, S.-I. A Comparative Study of Image Classification Method to Classify Onion and Garlic Using Unmanned Aerial Vehicle (UAV) Imagery. *Korean J. Soil Sci. Fertil.* **2016**, *49*, 743–750. [CrossRef]

27. Bannari, A.; Morin, D.; Bonn, F.; Huete, A.R. A review of vegetation indices. *Remote Sens. Rev.* **1995**, *13*, 95–120. [CrossRef]

28. Huete, A.; Jackson, R.; Post, D. Spectral response of a plant canopy with different soil backgrounds. *Remote Sens. Environ.* **1985**, *17*, 37–53. [CrossRef]

29. Huete, A.R. Soil influences in remotely sensed vegetation-canopy spectra. In *Theory and Applications of Optical Remote Sensing*; Asrar, G., Ed.; Wiley: New York, NY, USA, 1989; pp. 107–141.

30. Galvão, L.S.; Vitorello, Í. Variability of Laboratory Measured Soil Lines of Soils from Southeastern Brazil. *Remote Sens. Environ.* **1998**, *63*, 166–181. [CrossRef]

31. Nanni, M.R.; Demattê, J. Spectral Reflectance Methodology in Comparison to Traditional Soil Analysis. *Soil Sci. Soc. Am. J.* **2006**, *70*, 393–407. [CrossRef]

32. Chen, J.; Gu, S.; Shen, M.; Tang, Y.; Matsushita, B. Estimating aboveground biomass of grassland having a high canopy cover: An exploratory analysis of in situ hyperspectral data. *Int. J. Remote Sens.* **2009**, *30*, 6497–6517. [CrossRef]

33. Yoshioka, H.; Miura, T.; Demattê, J.A.M.; Batchily, K.; Huete, A.R. Derivation of Soil Line Influence on Two-Band Vegetation Indices and Vegetation Isolines. *Remote Sens.* **2009**, *1*, 842–857. [CrossRef]

34. Baret, F.; Jacquemoud, S.; Hanocq, J. About the soil line concept in remote sensing. *Adv. Space Res.* **1993**, *13*, 281–284. [CrossRef]

35. Park, J.K.; Park, J.H. Crops Classification Using Imagery of Unmanned Aerial Vehicle (UAV). *J. Korean Soc. Agric. Eng.* **2015**, *57*, 91–97. [CrossRef]

36. Xue, J.; Su, B. Significant Remote Sensing Vegetation Indices: A Review of Developments and Applications. *J. Sens.* **2017**, *2017*, 1–17. [CrossRef]

37. Lichtenthaler, H.K.; Lang, M.; Sowinska, M.; Heisel, F.; Miehé, J. Detection of Vegetation Stress via a New High Resolution Fluorescence Imaging System. *J. Plant Physiol.* **1996**, *148*, 599–612. [CrossRef]

38. Garbulsky, M.F.; Peñuelas, J.; Gamon, J.; Inoue, Y.; Filella, I. The photochemical reflectance index (PRI) and the remote sensing of leaf, canopy and ecosystem radiation use efficiencies: A review and meta-analysis. *Remote Sens. Environ.* **2011**, *115*, 281–297. [CrossRef]

39. Zhang, Q.; Chen, J.M.; Ju, W.; Wang, H.; Qiu, F.; Yang, F.; Fan, W.; Huang, Q.; Wang, Y.-P.; Feng, Y.; et al. Improving the ability of the photochemical reflectance index to track canopy light use efficiency through differentiating sunlit and shaded leaves. *Remote Sens. Environ.* **2017**, *194*, 1–15. [CrossRef]

40. Tucker, C.J. Red and photographic infrared linear combinations for monitoring vegetation. *Remote Sens. Environ.* **1979**, *8*, 127–150. [CrossRef]

41. Rouse, J.; Haas, R.; Schell, J.; Deering, D. *Monitoring Vegetation Systems in the Great Plains with ERTS*; NASA. Goddard Space Flight Center 3d ERTS-1 Symp.; 1973; Volume 1, pp. 309–317. Available online: http://hdl.handle.net/2060/19740022614 (accessed on 24 August 2020).

42. Louhaichi, M.; Borman, M.M.; Johnson, D.E. Spatially Located Platform and Aerial Photography for Documentation of Grazing Impacts on Wheat. *Geocarto Int.* **2001**, *16*, 65–70. [CrossRef]

43. Horler, D.N.H.; Dockray, M.; Barber, J. The red edge of plant leaf reflectance. *Int. J. Remote Sens.* **1983**, *4*, 273–288. [CrossRef]

Publisher's Note: MDPI stays neutral with regard to jurisdictional claims in published maps and institutional affiliations.